***The FASEB Journal*** express article 10.1096/fj.00-0719fje. Published online April 6, 2001.

# Amyloid β-peptide induces nitric oxide production in rat hippocampus: association with cholinergic dysfunction and amelioration by inducible nitric oxide synthase inhibitors

Manh Hung Tran,* Kiyofumi Yamada,* Ana Olariu, Makoto Mizuno,
Xiu Hai Ren, and Toshitaka Nabeshima

Department of Neuropsychopharmacology and Hospital Pharmacy, Nagoya University Graduate School of Medicine, Nagoya 466-8560, Japan

*These authors contributed equally to this work.

Corresponding author: Toshitaka Nabeshima, Department of Neuropsychopharmacology and Hospital Pharmacy, Nagoya University Graduate School of Medicine, Nagoya 466-8560, Japan. Email: tnabeshi@med.nagoya-u.ac.jp

## ABSTRACT

Amyloid β-peptide (Aβ) plays a critical role in the development of Alzheimer's disease. However, the molecular mechanisms of Aβ-induced brain damage *in vivo* remain to be elucidated. Here, we investigated whether overproduction of nitric oxide (NO) catalyzed by inducible NO synthase (iNOS) is involved in Aβ-induced brain dysfunction. Chronic intracerebroventricular infusion of Aβ1-40 induced iNOS mRNA expression in the hippocampus on days 3 and 5 after the infusion. An accumulation of NO metabolites was observed, and the peak correlated with expression of iNOS mRNA. Measurement of NOS activities revealed an increase in $Ca^{2+}$-independent, but not $Ca^{2+}$-dependent, activity. Immunohistochemistry identified numerous iNOS-immunoreactive microglia and astrocytes in the dentate gyrus and to a lesser extent in the CA1 subfield of the hippocampus. Daily treatment with the iNOS inhibitor aminoguanidine (AG, 100 mg/kg/day, i.p.) or *S*-methylisothiourea (10 mg/kg/day, i.p.) during Aβ infusion prevented an impairment of nicotine-evoked acetylcholine release induced by Aβ, whereas the neuronal NOS inhibitor 7-nitroindazole (30 mg/kg/day, i.p.) had no effect. Daily treatment with AG also ameliorated the impairment of spatial learning of Aβ-infused rats in a radial arm maze. Our findings suggest that overproduction of NO catalyzed by iNOS is responsible for Aβ-induced brain dysfunction.

Key words: amyloid β-peptide ▪ nitric oxide synthase ▪ Alzheimer's disease ▪ acetylcholine ▪ learning and memory

Alzheimer's disease (AD) is a neurodegenerative disorder characterized by the presence of senile plaques and neurofibrillary tangles in the brain accompanied by progressive loss of synapses, neurons, and cognitive function (1-3). Previously, we reported that continuous intracerebroventricular (i.c.v.) infusion of amyloid β-peptide (Aβ) into rats induced learning and memory impairment, neuronal and morphological alterations, and brain dysfunction

(4-7). Although much progress has been made in understanding this age-related neurodegenerative disorder, insight into the pathogenesis of the disease has required additional study.

Recently, an increasing amount of evidence has shown that oxidative reactions occur in AD and that Aβ may be one molecular link between oxidative stress and AD-associated neuronal cell death. The aggregation of Aβ can attract inflammatory mediators (8, 9) that, in turn, generate nitric oxide (NO) radicals. Together with inflammatory mediators, Aβ also stimulates NO production and expression of the high-output isoform, inducible nitric oxide synthase (iNOS), in mouse microglia (10) or in rat astrocytes (11, 12). This Aβ-induced iNOS expression can result in an overproduction of NO, which may react with $O_2^-$ to yield highly reactive peroxynitrite and may, therefore, increase the overall radical burden in Aβ-loaded brain regions (13-15). The widespread occurrence of peroxynitrite can lead to damage of neuronal cells in AD (16) and nitration of synaptic proteins (17), thus affecting signal transduction pathways of cellular regulation.

Neurodegeneration in AD affects primarily certain types of neurons, particularly those in the hippocampus. To determine whether NO is involved in Aβ-induced brain dysfunction *in vivo*, rats were continuously infused with Aβ1-40 into the cerebroventricular area, and expression of iNOS mRNA and protein at different time points in the hippocampus was then analyzed by reverse transcriptase-polymerase chain reaction (RT-PCR) and immunohistochemistry, respectively. The production of NO and the alteration of NOS activity in this region of the brain were also quantified by using an NO-detector high-pressure liquid chromatography (HPLC) system (18). Moreover, to ascertain the involvement of NO in the brain dysfunction of Aβ-infused rats, the effects of iNOS inhibitors on Aβ-induced impairment of acetylcholine (ACh) release and spatial learning were evaluated by microdialysis and a radial eight-arm maze (RAM) task, respectively. Our data suggest the involvement of an excess of NO synthesized by iNOS in the pathogenesis of Aβ-induced brain dysfunction.

## MATERIALS AND METHODS

### Animals and drug treatments

Male Wistar rats (Charles River, Yokohama, Japan) weighing 200-250 g at the beginning of the experiments were used. They were housed in groups of three or four animals under standard light-dark conditions (12 h light cycle starting at 9:00 AM) at a constant temperature of 23°C. The animals had free access to food and water. During the acclimatization period, they were handled in accordance with the guidelines established by the Institute for Laboratory Animal Research of Nagoya University, the Guiding Principles for the Care and Use of Laboratory Animals approved by the Japanese Pharmacological Society, and the National Institutes of Health Guide for the Care and Use of Laboratory Animals. The procedure for infusion of Aβ has been described previously (4). Briefly, an i.c.v. cannula attached to a mini-osmotic pump (ALZET 2002; Alza, Palo Alto, CA) was implanted in the right cerebral ventricle (AP −0.3 mm, L +1.2 mm, V +4.0 mm) according to the atlas of Paxinos and Watson (19). The Aβ fragment (BACHEM AG, Bubendorf, Switzerland) 1-40, 1-42, or 25-35 was continuously infused into the cerebral ventricle at a rate of 300 pmol/12 μl/day, or 3 nmol/12 μl/day for 10 days. The peptide was dissolved in 35% acetonitrile/0.1% trifluoroacetic acid. Control animals were infused with

the vehicle or nontoxic Aβ reverse fragment 40-1. Rats treated with NOS inhibitors received a single daily dose of either neuronal NOS (nNOS) inhibitor 7-nitroindazole (7-NI, 30 mg/kg, i.p., Sigma, St. Louis, MO) or iNOS inhibitor aminoguanidine (AG, 100 mg/kg, i.p., Sigma), or *S*-methylisothiourea (SMT, 10 mg/kg, i.p., Calbiochem, La Jolla, CA) for 10 days after the start of Aβ infusion.

**RT-PCR analysis of iNOS mRNA**

On days 1, 3, 5, and 7 after Aβ infusion, rats were decapitated. The brains were removed and dissected out. Total RNA in the hippocampus was extracted by using Trizol reagent (Life Technologies, Grand Island, NY) according to the manufacturer's procedure. The RNA (2.5 μg) was reverse transcripted using 200 U of RT (SuperScript II, Life Technologies) with 1.0 μl of random hexamer for 1 h at $42^0$C. After reverse transcription of RNA to cDNA, the cDNA was amplified by PCR. For iNOS mRNA, the following primers (Katayama, Nagoya, Japan) were used: a sense primer, 5'-GGGGAGCAGGGCCACCTCTATGTTT-3', corresponding to the nucleotide sequence 3313-3337 of rat iNOS mRNA (20) and an anti-sense primer, 5'-GAGTCTTGTGCCTTTGGGCTCCTCC-3', corresponding to the nucleotide sequence 3520-3544. The reaction mixture for PCR amplification consisted of 1 μl of RT product, 10 pmol of each primer, and diethylpyrocarbonate-treated water in a total volume of 25 μl. The PCR was performed with a Perkin-Elmer Thermal Reactor for 30 cycles ($94^O$C for 1 min, $59^O$C for 1 min, and $72^O$C for 1 min). To assess the variability in mRNA content, β-actin mRNA was also amplified. After RT-PCR, 10 μl aliquots of the samples were subjected to 1.5% agarose gel electrophoresis at 100 V and stained with ethidium bromide. After electrophoresis was completed, the gel was exposed to UV light (Gel Doc 1000, Bio-Rad, Hercules, CA). The gel contained a 234 base pair (234 bp) band for the iNOS gene. The level of iNOS mRNA was expressed as a ratio to that of β-actin mRNA.

**Measurement of NO metabolites**

NO production in the brain was assessed by the simultaneous measurement of its metabolites $NO_2^-$ and $NO_3^-$ (18). In brief, rat brain was dissected, after which the hippocampus was rapidly frozen and stored in a deep freezer at $-80^O$C until the assay. The hippocampus was homogenized in 10 volumes (wt/vol) of 50 mM Tris-HCl buffer (pH 7.4) containing 0.1 mM EDTA, 0.1 mM phenylmethylsulfonyl fluoride, and 10 μg/ml aprotinin. The homogenates were centrifuged at 30,000*g* for 30 min, and supernatants were used in the assay. The supernatant (equal to 20 μg of cytosolic protein) was injected into an automatic NO detector-HPLC system (ENO-10, Eicom, Kyoto, Japan). The $NO_2^-$ and $NO_3^-$ in the supernatant were separated in a reverse phase separation column packed with polystyrene polymer (NO-PAK, 4.6 × 50 mm, Eicom), and $NO_3^-$ was reduced to $NO_2^-$ in a reduction column packed with copper-plated cadmium filings (NO-RED, Eicom). $NO_2^-$ was mixed with Griess reagent to form a purple azo dye in a reaction coil. The separation and the reduction columns were placed in a column oven that was set at $35^O$C. The absorbance of the color of the product dye at 540 nm was measured by a flow-through spectrophotometer (NOD-10, Eicom). The mobile phase, which was delivered by a pump at a rate of 0.33 ml/min, was 10% methanol containing 0.15 M NaCl/$NH_4$Cl and 0.5 g/L 4Na-EDTA. The Griess reagent, which was 1.25% HCl containing 5 g/L sulfanilamide with 0.25 g/L *N*-naphthylethylenediamine, was delivered at a rate of 0.1 ml/min. Contamination by $NO_2^-$ and $NO_3^-$ of the homogenate buffer and the reliability of the reduction column were examined in

each experiment.

**Assay of NOS activity**

NOS activity was assayed by measuring the production of $NO_x^-$ ($NO_2^-$ plus $NO_3^-$) as described previously (21). The hippocampus was homogenized in 10 volumes (wt/vol) of 50 mM Tris-HCl buffer (pH 7.4) containing 0.1 mM EDTA, 0.1 mM phenylmethylsulfonyl fluoride, and 10 μg/ml aprotinin. The homogenates were centrifuged at 30,000*g* for 30 min, and the supernatants were used in the assay. The supernatants were incubated for 30 min at either 4 or 37°C in a final volume of 200 μl, containing 2 mM $CaCl_2$, 0.1 mM EDTA, 0.1 mM L-arginine, 0.04 mM flavin adenine dinucleotide, 0.05 mM tetrahydrobiopterin, and 0.05 mM flavin mononucleotide. The reaction was terminated by addition of 50 μl of 0.1 mM perchloric acid, and the samples were centrifuged at 30,000*g* for 20 min. $NO_x^-$ levels in the supernatants were measured using the NO detector-HPLC system as described above. NOS activity was determined as the difference between $NO_x^-$ levels in the samples incubated at 37 and 4°C. $Ca^{2+}$-independent activity was measured as the activity of iNOS, by replacing 2 mM $CaCl_2$ with EGTA in the assay mixture. $Ca^{2+}$-dependent activity was defined as the difference in the activity measured in the presence and absence of $CaCl_2$ and was regarded as constitutive NOS activity. Protein content was determined according to the method of Lowry et al. (22) with bovine serum albumin as a standard.

**Immunohistochemistry**

On day 5 after Aβ infusion, rats were deeply anesthetized with pentobarbital and transcardiac perfusion with physiological saline was performed, followed by 4% paraformaldehyde in 100 mM phosphate-buffered saline (PBS, pH 7.4). After perfusion, the brains were quickly removed and were postfixed at 4°C for 24 h in the same fixative solution. The brains were then cryoprotected in a 20% sucrose solution in 100 mM PBS at 4°C for 12 h and further in a 40% sucrose solution in 100 mM PBS at 4°C for at least 24 h. Sections were cut 30 μm thick in a cryostat and collected in 100 mM PBS containing 0.3% Triton X-100. After several washes, the free-floating sections were incubated with primary mouse monoclonal antibody against iNOS (diluted 1:250, Transductions Laboratories, Lexington, KY) for 48 h at 4°C. For double immunostaining, the primary mouse monoclonal antibody against iNOS was incubated together with either rabbit anti-glial fibrillary acidic protein (GFAP) polyclonal antibody (1:500, Chemicon International, Temecula, CA) or rat anti-mouse CD11b (Mac-1) monoclonal antibody (1:500, Chemicon International). The sections were then incubated with rabbit anti-mouse immunoglobulin G (IgG)-conjugated fluorescein-5-isothiocyanate (1:200, Cappel, Aurora, OH) alone or together with either anti-rabbit IgG-conjugated rhodamine (1:500, Chemicon International) or goat anti-rat IgG-conjugated Texas red (1:500, Molecular Probes, Eugene, OR) for 3 h at room temperature. After each incubation, all sections were washed several times with PBS. Finally, they were mounted on a glass slide and a coverslip with Entellan was placed.

**Microdialysis and determination of ACh release**

Ten days after the start of infusion of Aβ, the cannula delivering Aβ was removed and a dialysis probe for the measurement of ACh release was implanted (5). Briefly, rats were anesthetized with pentobarbital (30 mg/kg, i.p.) and fixed in a stereotaxic frame. A dialysis probe (A-I-8-03;

membrane length 3 mm, EICOM, Kyoto, Japan) was implanted into a region extending from the frontoparietal cortex to the hippocampus [AP −3.8; L +2.2; V +1.0-4.0 mm (19)], because deposition of Aβ was observed in the frontal cortex and hippocampus around the ventricle (4). About 24 h after the implantation of the dialysis probe, Ringer's solution (147 mM NaCl, 4 mM KCl, and 2.3 mM $CaCl_2$) containing $10^{-5}$ M eserin was perfused at a flow rate of 2.0 μl/min, and dialysate was collected every 15 min and analyzed by HPLC with electrochemical detection (ECD). Details of the measurement of ACh by HPLC-ECD have been described previously (23).

**RAM task**

The effects of Aβ1-40 infusion and iNOS inhibitors on spatial reference and working memory task were assessed by using an RAM (24, 25). The maze consisted of eight arms (No.1 to No. 8; 48 × 12 cm) extending radially from a central area (32 cm in diameter), with a 5 cm edge around the apparatus. The floor of the arms and central area was painted black. The apparatus was placed 40 cm above the floor and was surrounded by various extramaze cues such as a laboratory bench, posters, and a clock. The extramaze cues were placed at the same position during the study. At the end of each arm there was a food cup that held a single 50 mg food pellet. After Aβ infusion and prior to the performance of the RAM task, the animals were kept on a restricted diet, and body weight was maintained at 85 % of the free-feeding weight for 6 days, with water being available *ad libitum*. Before the actual training began, the animals in groups of four had a shaping period of 4 days to explore the arms and consume the baits. The baits were initially available throughout the maze but were gradually restricted to the food cups. Following this shaping period, each animal was placed individually in the center of the maze and subjected to the maze training. Rats underwent five consecutive training trials at 5 min intervals, every day for 5 days, which continued until all four baits in the food cups had been consumed or until 5 min had elapsed. Working memory was measured by counting the number of entries into an arm containing food but previously visited; reference memory was assessed by counting the number of entries into unbaited arms. The time spent in each arm to collect a bait was also measured as an index of locomotor function.

**Statistical analyses**

The results are expressed as means ± SE. Statistical significance in the neurochemical experiments was determined by one-way ANOVA, followed by the two-tailed Bonferroni test for multigroup comparison, or the Wilcoxon test or Student's *t* test (two-group comparison). An ANOVA with repeated measures, followed by the two-tailed Bonferroni test or the Student-Newman-Keuls test for multigroup comparison, was utilized in the behavioral experiments. A *P* value less than 0.05 was regarded as statistically significant.

## RESULTS

**Effect of Aβ1-40 infusion on iNOS mRNA expression analyzed by RT-PCR**

In AD patients, the expression of iNOS mRNA in a subset of pyramidal neurons of the hippocampus (26) and in tangle-bearing neurons (27) has been reported. To investigate whether Aβ can induce this effect in experimental animals *in vivo*, rats were continuously infused i.c.v. with Aβ1-40 and examined for the expression of iNOS mRNA by RT-PCR at different time

points. In naive and control rats infused with Aβ40-1, bands were almost undetectable, whereas in Aβ1-40-treated rats there were specific bands as expected (Fig. 1A). The specific bands of iNOS cDNAs visualized by agarose gel electrophoresis were quantified relative to β-actin. As shown in Fig. 1B, the expression of iNOS mRNA was time dependent. One day after the start of Aβ infusion, an increase in iNOS gene expression was observed in both Aβ1-40-infused rats and Aβ40-1-infused control rats, and no significant difference between the two groups was observed. On days 3 and 5 after Aβ infusion, a significant increase in iNOS expression was evidenced in rats receiving Aβ1-40, indicating that infusion of the active peptide induced iNOS expression *in vivo*. On day 7, expression of iNOS returned to the basal level.

**Effects of Aβ1-40 infusion on NO production and NOS activity**

Although the increase in iNOS mRNA expression was evident in Aβ-infused rats, it is worth establishing whether this can result in an increase in NOS activity and NO production. NO production in the hippocampus was significantly enhanced in Aβ1-40-treated rats, as evidenced by an increased tissue level of NO metabolites. The production of NO peaked on days 3 and 5 after Aβ infusion and correlated well with the iNOS mRNA expression data. On day 7, NO production returned to the basal level (Fig. 2A). Daily treatment with AG (100 mg/kg, i.p.), an iNOS inhibitor, in Aβ1-40-infused rats abolished the increase in NO metabolite contents in the hippocampus on days 3 and 5, suggesting that NO formation was catalyzed by the iNOS (Fig. 2A).

Because iNOS activity is $Ca^{2+}$ independent but nNOS activity is $Ca^{2+}$ dependent, we also examined by which isoform NO was synthesized after Aβ infusion. Because of the results of iNOS expression and NO production studies, we measured $Ca^{2+}$-dependent and $Ca^{2+}$-independent NOS activity on days 3 and 5 after Aβ infusion. As shown in Fig. 2B, there was a pronounced increase in $Ca^{2+}$-independent NOS activity in Aβ1-40-treated rats when compared with control rats, whereas $Ca^{2+}$-dependent NOS activity was not altered. These findings further supported the previous results for iNOS mRNA expression and indicated that iNOS acts continuously to produce a large amount of NO.

**Immunohistochemistry of iNOS-positive cells**

The expression of the iNOS isoform at early postlesion stages is associated with the activation of glia (28); thus, we used immunohistochemical staining with mouse monoclonal antibody against iNOS to identify the localization of iNOS protein. Because the expression of iNOS mRNA was previously shown to peak at days 3 and 5 after Aβ infusion, immunohistochemical staining was performed on day 5 after the start of Aβ infusion. Immunohistochemical staining with anti-iNOS antibody and fluorescent microscopy revealed an abundance of immunoreactive cells in the dentate gyrus and to a lesser extent in the CA1 subfield of the hippocampus in Aβ1-40-infused rats (Fig. 3B) compared with control rats (Fig. 3A). Double labeling for markers of microglia (anti-CD11b antibody) and astrocytes (anti-GFAP antibody) in combination with the iNOS antibody demonstrated that iNOS-immunoreactive cells (green) colocalized with both CD11b-immunopositive cells (red) (Fig. 3C) and GFAP-immunopositive cells (orange) (Fig. 3D). These results indicated that iNOS was expressed in both microglia and astrocytes.

**Effects of various Aβ fragments on nicotine-evoked ACh release and the ameliorating**

**effect of iNOS inhibitors *in vivo***

Excessive production of NO catalyzed by iNOS may lead to neurotoxicity (29-31). Because we have previously demonstrated that continuous infusion of Aβ impaired learning and memory and caused brain dysfunction (6, 7), a possible link between NO overproduction and brain dysfunction induced by Aβ was investigated. First, we examined the effects of various Aβ fragments on ACh release *in vivo* (5). We used a microdialysis technique to quantify ACh release under nicotine stimulation. As shown in Fig. 4A, no alteration of nicotine-evoked ACh release was observed among naive rats, vehicle-treated rats, and Aβ40-1-infused rats. However, continuous infusion of neurotoxic Aβ fragments, including Aβ1-42 and Aβ1-40, at 300 pmol/day resulted in a significant attenuation in nicotine-stimulated ACh release compared with that in naive rats or rats receiving either vehicle or the nontoxic reverse fragment Aβ40-1 (Fig. 4B). The maximum effect of nicotine that evoked ACh release was at 30 min after the infusion and resembled the effect found in our previous study (5). Aβ25-35 at 3 nmol/day, but not 300 pmol/day, also impaired the nicotine-evoked ACh release when compared with vehicle (data not shown). There was no significant difference in the basal extracellular ACh level among groups (see legend of Fig. 4A).

To investigate whether NO is involved in the impairment of the nicotine-evoked ACh release after Aβ infusion, rats were injected daily with a single dose of the iNOS inhibitor AG (100 mg/kg., i.p.) or SMT (10 mg/kg, i.p.) or the nNOS inhibitor 7-NI (30 mg/kg., i.p.) for 10 days. Daily treatment with 7-NI, which inhibits nNOS by 60% without affecting blood pressure (32), failed to prevent the impairment of nicotine-evoked ACh release (data not shown). Daily treatment with AG or SMT led to recovery of the impairment of ACh release after nicotine stimulation without affecting the basal release (Fig. 5A). However, daily treatment with AG or SMT in rats infused with vehicle or Aβ40-1 did not produce any alteration in nicotine-evoked ACh release (data not shown). Coadministration of L-arginine (L-Arg, 200 mg/kg, i.p.), an NO precursor, eliminated the recovery of nicotine-stimulated ACh release induced by AG (Fig. 5B), thus providing evidence that iNOS inhibitors could ameliorate the Aβ-induced impairment of nicotine-evoked ACh release *in vivo*.

**Prevention of Aβ-induced impairment of spatial learning by iNOS inhibitor**

As described in Materials and Methods, the effect of Aβ1-40 infusion on spatial reference and working memory was assessed with an RAM. By counting the number of working errors and reference errors, spatial memory can be evaluated and compared among groups of animals. An ANOVA with repeated measures of total number of errors among the three groups (Fig. 6A) revealed significant effects of group ($F_{(2,21)}$ = 6.431; $P$ < 0.01) and trial ($F_{(4,84)}$ = 54.514; $P$<0.0001) but not group by trial interaction ($F_{(8,84)}$ = 0.735; $P$ = 0.66). Post-hoc analysis with the Bonfferoni test indicated that Aβ1-40 significantly impaired spatial memory formation ($P$<0.01), which was markedly prevented by treatment with AG ($P$<0.005). No difference in time spent per trial in the arms was found among groups (Fig. 6B), indicating that the effects of Aβ1-40 and AG on maze performance are not due to alteration of locomotor function.

To elucidate which memory category was impaired by Aβ, total memory errors were divided into reference and working memory errors. Repeated measure ANOVA indicated significant effects of group on both working memory ($F_{(8,81)}$ = 4.481; $P$<0.05, Fig. 6C) and reference

memory ($F_{(8,81)}$ = 6.834; $P$<0.01, Fig. 6D) errors. Post-hoc analysis with the Bonfferoni test showed that working ($P$<0.05) and reference ($P$<0.05) memory formation was significantly impaired by Aβ1-40 and that AG significantly prevented Aβ-induced impairment of working ($P$<0.05) and reference ($P$<0.002) memory.

## DISCUSSION

Here we have demonstrated that continuous infusion of Aβ1-40 into rat cerebral ventricle induced a time-dependent expression of iNOS in the dentate gyrus of the hippocampus. The abilities of Aβ1-40 or Aβ1-42 to stimulate iNOS expression in rat striatum (28) or in rat cortical glial cultures (11, 12) have been reported previously. However, it appears that differences in experimental conditions *in vivo* and/or *in vitro* may lead to different patterns of iNOS expression. In our experiments, rats received continuous i.c.v. infusions with 300 pmol/day of soluble Aβ1-40, which has been shown to cause Aβ deposition in the hippocampus and frontal cortex (4), and the peak of iNOS expression was detected on days 3 to 5 after Aβ infusion. In rat cortical glial cultures, a higher dose (10 μM) of an aggregated form of Aβ1-42 results in a rapid expression of iNOS (after 6 h, with a peak at 36 h) (12). A single injection of either soluble or fibrillar Aβ1-40 into rat striatum also increases the number of iNOS-immunoreactive cells surrounding the needle track, but much delayed (at day 30 after injection) (28). Aβ is constitutively produced in cells (33), and soluble Aβ is present at nanomolar concentrations in biological fluids of normal and AD-inflicted individuals (34). Thus, the delayed effect of Aβ in inducing iNOS expression in our experiment may be attributed to the gradual accumulation of a sufficiently toxic level of Aβ. However, expression of iNOS mRNA is transient, even in the presence of continuous Aβ. This phenomenon may be due to an instability of the iNOS mRNA and/or an inhibition of transcriptional induction of iNOS by NO, as reported elsewhere (35, 36), because on day 7 iNOS mRNA returned to the basal level. It is worth noting that under our experimental conditions, an i.c.v. infusion of Aβ induced iNOS expression in both the ipsilateral and the contralateral hippocampus. A single injection of the peptide (28) or lipopolysacharide (31, 37), however, stimulated mainly iNOS expression around the injection site. Thus, i.c.v. infusion seems to exert a global effect of Aβ. The slight expression of iNOS in rats infused with Aβ40-1 may be due to the operative procedure used for i.c.v. cannula implantation, which may provoke an inflammatory response. Immunohistochemistry further revealed the localization of iNOS-immunoreactive cells in the dentate gyrus and CA1 subfield of the hippocampus. The expression of iNOS was found in both microglia and astrocytes, suggesting an activation of glial cells by Aβ. These results agree with those of other reports (12, 37, 38). The robust expression of iNOS in the dentate gyrus implies that this subregion of the hippocampus is most susceptible to Aβ toxicity under our experimental conditions. Following the iNOS expression, $Ca^{2+}$-independent NOS activity and $NO_x^-$ production also increased with the same pattern, further supporting the finding that Aβ stimulates NO production.

Previously, we demonstrated that infusion of Aβ1-40 impairs nicotine-evoked ACh and dopamine release in the frontal cortex/hippocampus and the striatum, respectively (5). Infusion of Aβ1-42, however, decreased the affinity of nicotinic ACh receptor in the hippocampus (39). In the present study, infusion with various Aβ fragments (1-40, 1-42, or 25-35) also impaired nicotine-evoked ACh release, thus confirming that Aβ impairs signal transduction via the nicotinic ACh receptor. It has been reported that Aβ binds to receptor for advanced glycation

end-products and/or scavenger receptors on microglia and may induce cell death by generating free radicals including NO (40). Evidence is accumulating that an inappropriate formation of NO synthesized by iNOS may cause neurotoxicity (31, 41-43). In our experiments, iNOS inhibitors such as AG and SMT reversed the impairment of nicotine-evoked ACh release, thus implicating the involvement of NO in the Aβ-induced dysfunction of nicotinic ACh receptor signaling and the ameliorating effects of iNOS inhibitors. The effect of iNOS inhibitors in ameliorating the impairment of nicotine-evoked ACh release is specific because: a) both AG and SMT are iNOS-specific inhibitors (44, 45); b) coadministration of the iNOS inhibitor AG and the NO precursor L-arginine eliminates the ameliorating effect of AG; and c) AG or SMT treatment in control rats does not alter nicotine-evoked ACh release. Ameliorating effects of iNOS inhibitors in experiments on central nervous system pathophysiology such as cerebral ischemic damage (46), cerebral artery occlusion (47), and lipopolysaccharide-induced neurotoxicity (31) have also been demonstrated. In contrast to iNOS inhibitors, the nNOS inhibitor 7-NI failed to ameliorate nicotine-evoked ACh release. Although only one nNOS inhibitor was used, the result seems to be consistent with the fact that $Ca^{2+}$-dependent activities did not change. Accordingly, it is unlikely that NO synthesized by nNOS participates in the Aβ-induced cholinergic dysfunction under our experimental conditions. The mechanism of the NO involvement in this regard needs to be defined; however, the formation of peroxynitrite (16) or the nitration of synaptic proteins (17) may affect signal transduction pathways of cellular regulation.

It has been believed that cholinergic dysfunction is one of the primary causes of cognitive deficits in AD patients (48). Previously, we found that continuous i.c.v. infusion of Aβ1-40 or Aβ1-42 led to the impairment of spatial memory formation in a water maze in an animal model (4, 49). We showed here that continuous i.c.v. infusion of Aβ1-40 also impaired the spatial reference and working memory performance in the RAM. It is interesting that AG, an iNOS inhibitor, which is able to reduce the impairment of nicotine-evoked ACh release, also exerts an ameliorating effect on memory performance. Thus, it may be suggested that NO synthesized by iNOS contributes to the toxic effect of Aβ on brain dysfunction. The ameliorating effect of AG on memory performance is not attributable to the enhancement of motility, because the time spent in the arms of the maze did not differ among the groups.

In contrast to the NO synthesized by nNOS, which facilitates learning and memory formation under physiological conditions (50-53), the NO synthesized by iNOS under our experimental conditions is deleterious. We showed that iNOS activity and NO production were markedly increased after 3-5 days of Aβ1-40 infusion. That iNOS produced a large amount of NO, which may cause neurotoxicity *in vitro*, has been previously reported (42, 43). The impairment of nicotine-evoked ACh release and memory performance was observed after 10 days of Aβ1-40 infusion, and therefore these manifestations may be attributable to the delayed neurotoxic effect of NO. In conclusion, we suggest that chronic i.c.v. infusion of Aβ1-40 induces iNOS expression *in vivo*, which produces neurotoxic levels of NO and results in cholinergic signaling dysfunction and memory impairment. Treatment with iNOS inhibitors can ameliorate the cholinergic dysfunction and the memory performance, thus implying a therapeutic strategy for AD.

## ACKNOWLEDGMENTS

This study was supported in part by Grants-in-Aid for Science Research (No. 99187 and No. 12210075); by a COE Grant from the Ministry of Education, Science, Sports and Culture of

Japan; by Special Coordination Funds for the Promotion of Science and Technology, Target-oriented Brain Science Research Program, from the Ministry of Science and Technology of Japan; and by an SRF Grant for Biomedical Research. We are very grateful to Dr. Masayuki Hiramatsu for his technical assistance with the fluorescent image processing.

## REFERENCES

1. Glenner, G.G. (1988) Alzheimer's disease: its proteins and genes. *Cell* **52**, 307-308

2. Kang, J., Lemaire, H., Unterbeck, A., Salbaum, J., Masters, C., Grzeschick, K., Multhaup, G., Beyreuther, K., and Muller, H.B. (1987) The precursor of Alzheimer's disease amyloid A4 protein resembles a cell-surface receptor. *Nature* **325**, 733-736

3. Braak, H., and Braak, E. (1991) Demonstration of amyloid deposits and neurofibrillary changes in whole brain sections. *Brain Pathol.* **1**, 213-216

4. Nitta, A., Itoh, A., Hasegawa, T., and Nabeshima T. (1994) β-Amyloid protein-induced Alzheimer's disease animal model. *Neurosci. Lett*. **170**, 63-66

5. Itoh, A., Nitta, A., Nadai, M., Nishimura, K., Hirose, M., Hasegawa, T., and Nabeshima T. (1996) Dysfunction of cholinergic and dopaminergic neuronal systems in β-amyloid protein-infused rats. *J. Neurochem*. **66**, 1113-1117

6. Nabeshima, T., and Itoh, A. (1997) Toxicity of β-amyloid protein: neurochemical, histological and behavioral changes. In *Alzheimer's Disease: Biology, Diagnosis and Therapeutics* (Iqbal, K., Winblad, B., Nishimura, T., Takeda, M., and Wisniewski, H.M., eds.), pp. 623-630, John Wiley & Sons, Chichester, U.K.

7. Yamada, K., and Nabeshima, T. (2000) Animal model of Azheimer's disease and evaluation of anti-dementia drugs. *Pharmacol. Ther*. In press

8. Yates, S.L., Burgess, L.H., Kocsis-Angle, J., Antal, J.M., Dority, M.D., Embury, P.B., Piotrkowski, A.M., and Brunden, K.R. (2000) Amyloid beta and amylin fibrils induce increases in proinflammatory cytokine and chemokine production by THP-1 cells and murine microglia. *J. Neurochem.* **74**, 1017-1025

9. Galimberti, D., Baron, P., Meda, L., Prat, E., Scarpini, E., Delgado, R., Catania, A., Lipton, J.M., and Scarlato, G. (1999) Alpha-MSH peptides inhibit production of nitric oxide and tumor necrosis factor-alpha by microglial cells activated with beta-amyloid and interferon gamma. *Biochem. Biophys. Res. Commun.* **263**, 251-256

10. Meda, L., Cassatella, M.A., Szendrei, G.I., Otvos, L., Baron, P., Villalba, M., Ferrari, D., and Rossi, F. (1995) Activation of microglial cells by beta-amyloid protein and interferon-gamma. *Nature* **374**, 647-650

11. Akama, K.T., Albanese, C., Pestell, R.G., and Eldik, L.J.V. (1998) Amyloid beta-peptide stimulates nitric oxide production in astrocytes through an NFkappaB-dependent mechanism.

*Proc. Natl. Acad. Sci. USA* **95**, 5795-5800

12. Akama, K.T., and Eldik, L.J.V. (2000) Beta-amyloid stimulation of inducible nitric-oxide synthase in astrocytes is interleukin-1beta- and tumor necrosis factor-alpha (TNFalpha)-dependent, and involves a TNFalpha receptor-associated factor- and NFkappaB-inducing kinase-dependent signaling mechanism. *J. Biol. Chem.* **275**, 7918-7924

13. Beckman, J.S. (1994) Peroxynitrite versus hydroxyl radical: the role of nitric oxide in superoxide-dependent cerebral injury. *Ann. N. Y. Acad. Sci.* **738**, 69-75

14. Beckman, J.S., and Koppenol, W.H. (1996) Nitric oxide, superoxide, and peroxynitrite: the good, the bad, and ugly. *Am. J. Physiol*. **271**, C1424-C1437

15. McGeer, P.L., and McGeer, E.G. (1995) The inflammatory response system of brain: implications for therapy of Alzheimer and other neurodegenerative diseases. *Brain Res. Rev*. **21**, 195-218

16. Smith, M.A., Harris, P.L.R., Sayre, L.M., Beckman, J.S. and Perry, G. (1997) Widespread peroxynitrite-mediated damage in Alzheimer's disease. *J. Neurosci.* **17**, 2653-2657

17. Di Stasi, A.M., Mallozzi, C., Macchia, G., Petrucci, T.C., and Minetti, M. (1999) Peroxynitrite induces tryosine nitration and modulates tyrosine phosphorylation of synaptic proteins. *J. Neurochem*. **73**, 727-735

18. Yamada, K., and Nabeshima T. (1997) Simultaneous measurement of nitrite and nitrate levels as indices of nitric oxide release in the cerebellum of conscious rats. *J. Neurochem.* **68**, 1234-1243

19. Paxinos, G., and Watson, C. (1986) *The Rat Brain in Stereotaxic Coordinates*, 2nd ed, Academic Press, New York

20. Adachi, H., Iida, S., Oguchi, S., Ohshima, H., Suzuki, H., Nagasaki, K., Kawasaki, H., Sugimura, T., and Esumi, H. (1993) Molecular cloning of a cDNA encoding an inducible calmodulin-dependent nitric-oxide synthase from rat liver and its expression in COS 1 cells. *Eur. J. Biochem.* **217**, 37-43

21. Han, D., Yamada, K., Senzaki, K., Xiong, H., Nawa, H., and Nabeshima, T. (2000) Involvement of nitric oxide in pentylenetetrazole-induced kindling in rats. *J. Neurochem.* **74**, 792-798

22. Lowry, O.H., Rosebrough, N.J., Farr, A.L., and Randall R.J. (1951) Protein measurement with the Folin phenol reagent. *J. Biol. Chem*. **193**, 265-275

23. Hasegawa, M., Kinoshita, H., Amano, M., Hasegawa, T., Kameyama, T., and Nabeshima T. (1993) MK-801 increases endogenous acetylcholine release in the rat parietal cortex: a study using brain microdialysis. *Neurosci. Lett*. **150**, 53-56

24. Zou, LB., Yamada, K., Tanaka, T., Kameyama, T., and Nabeshima, T. (1998) Nitric oxide

synthase inhibitors impair reference memory formation in a radial arm maze task in rats. *Neuropharmacology* **37**, 323-330

25. Zou, LB., Yamada, K., Sasa, M., and Nabeshima, T. (1999) Two phases of behavioral plasticity in rats following unilateral excitotoxic lesion of the hippocampus. *Neuroscience* **92**, 819-826

26. Lee, S.C., Zhao, M.L., Hirano, A., and Dickson, D.W. (1999) Inducible nitric oxide synthase immunoreactivity in the Alzheimer disease hippocampus: association with Hirano bodies, neurofibrillary tangles, and senile plaques. *J. Neuropathol. Exp. Neurol.* **58**, 1163-1169

27. Vodovotz, Y., Lucia, M.S., Flanders, K.C., Chesler, L., Xie, Q.W., Smith, T.W., Weidner, J., Mumford, R., Webber, R., Nathan, C., Roberts, A.B., Lippa, C.F., and Sporn, M.B. (1996) Inducible nitric oxide synthase in tangle-bearing neurons of patients with Alzheimer's disease. *J. Exp. Med.* **184**, 1425-1433

28. Weldon, D.T., Rogers, S.D., Ghilardi, J.R., Finke, M.P., Cleary, J.P., O'Hare, E., Esler, W.P., Maggio, J.E., and Mantyh, P.W. (1998) Fibrillar beta-amyloid induces microglial phagocytosis, expression of inducible nitric oxide synthase, and loss of a select population of neurons in the rat CNS in vivo. *J. Neurosci*. **18**, 2161-2173

29. Mackenzie, G.M., Jackson, M.J., Jenner, P., and Marsden, C.D. (1997) Nitric oxide synthase inhibition and MPTP-induced toxicity in the common marmoset. *Synapse* **26**, 301-316

30. Dawson, V.L, Dawson, T.M. (1998) Nitric oxide in neurodegeneration. *Prog. Brain Res.* **118**, 215-229

31. Yamada, K., Komori, Y., Tanaka, T., Senzaki, K., Nikai, T., Sugihara, H., Kameyama, T., and Nabeshima, T. (1999) Brain dysfunction associated with an induction of nitric oxide synthase following an intracerebral injection of lipopolysaccharide in rats. *Neuroscience* **88**, 281-294

32. MacKenzie, G.M., Rose, S., Bland-Ward, P.A., Moore, P.K., Jenner, P., Marsden, C.D. (1994) Time course of inhibition of brain nitric oxide synthase by 7-nitroindazole. *Neuroreport* **5**, 1993-1996

33. Haass, C., Sclossmacher, M.G., Hung, A.Y., Vigo-Pelfrey, C., Mellon, A., Ostaszewski, B.L., Lieberburg, I., Koo, E.H., Schenk, D., Teplow, B.D., and Selkoe, D.J. (1992) Amyloid beta-peptide is produced by cultured cells during normal metabolism. *Nature* **359**, 322-325

34. Seubert, P., Vigo-Pelfrey, C., Esch, F., Lee, M., Dovey, H., Davis, D., Sinha, S., Sclossmacher, M., McCormack, R., Wolfert, R., Selkoe, D., Lieberburg, I., and Schenk, D. (1992) Isolation and quantification of soluble Alzheimer's beta-peptide from biological fluids. *Nature* **359**, 325-327

35. Park, S.K., Lin, H.L, and Murphy, S. (1994) Nitric oxide limits transcriptional induction of nitric oxide synthase in CNS glial cells. *Biochem. Biophys. Res. Commun.* **201**, 762-768

36. Park, S.K., and Murphy, S. (1996) Nitric oxide synthase type II mRNA stability is translation- and transcription-dependent. *J. Neurochem*. **67**, 1766-1769

37. Kitamura, Y., Takahashi, H., Matsuoka, Y., Toyama, I., Kimura, H., Nomura, Y., and Taniguchi, T. (1996) In vivo induction of inducible nitric oxide synthase by microinjection with interferon-gamma and lipopolysaccharide in rat hippocampus. *Glia* **18**, 233-243

38. Minghetti, L., Nicolini, A., Polazzi, E., Maclouf, J., and Levi, G. (1997) Inducible nitric oxide synthase expression in activated rat microglial cultures is down regulated by exogenous prostaglandin $E_2$ and by cyclooxygenase inhibitors. *Glia* **19**, 152-160

39. Olariu A., Kawahara, M., Yamada, K., Miyamoto, Y., and Nabeshima T. (1999) Alterations of nicotinic cholinergic receptor binding induced by beta-amyloid (1-42) in rats. *Soc. Neurosci. Abstr*. **25**, 2118

40. Mattson, M.P. (1997) Cellular actions of β-amyloid precursor protein and its soluble and fibrillogenic derivatives. *Physiol. Rev*. **77**, 1081-1131

41. Merrill, J.E., Ignarro, L.J., Sherman, M.P., Melinek, J., and Lane, T.E. (1993) Microglial cell cytotoxicity of oligodendrocytes is mediated through nitric oxide. *J. Immunol.* **151**, 2132-2141

42. Dawson, T.M., Dawson, V.L., and Snyder, S.H. (1994) Molecular mechanisms of nitric oxide actions in the brain. *Ann. N. Y. Acad. Sci.* **738**, 76-85

43. Hewett, S.J., Csernansky, C.A., and Choi, D.W. (1994) Selective potentiation of NMDA-induced neuronal injury following induction of astrocytic iNOS. *Neuron* **13**, 487-494

44. Griffiths, M.L.D., Messent, M., MacAllister, R.J., and Evans, T.W. (1993) Aminoguanidine selectively inhibits inducible nitric oxide synthase. *Br. J. Pharmacol.* **110**, 963-968

45. Szabo, C., Southan, G.J., and Thiemermann, C. (1994) Beneficial effects and improved survival in rodent models of septic shock with *S*-methylisothiourea sulfate, a potent and selective inhibitor of inducible nitric oxide synthase. *Proc. Natl. Acad. Sci. USA* **91**, 12472-12476

46. Iadecola, C., Zhang, F., and Xu, X. (1995) Inhibition of inducible nitric oxide synthase ameliorates cerebral ischemic damage. *Am. J. Physiol*. **268**, R286-R292

47. Zhang, F., Casey, R., Ross, E., and Iadecola, C. (1996) Aminoguanidine ameliorates and L-arginine worsens brain damage from intraluminal middle cerebral artery occlusion. *Stroke* **27**, 317-323

48. Coyle, J.T., Price, D.L., and Delong, M.R. (1983) Alzheimer's disease: a disorder of central cholinergic innervation. *Science* **219**, 1184-1190

49. Yamada, K., Tanaka, T., Han, D., Senzaki, K., Kameyama, T., and Nabeshima, T. (1999) Protective effects of idebenone and α-tocopherol on β-amyloid-(1-42)-induced learning and memory deficits in rats: implication of oxidative stress in β-amyloid-induced neurotoxicity in vivo. *Eur. J. Neurosci*. **11**, 83-90

50. Böhme, G.A., Bon, C., Lemaire, M., Reibaud, M., Piot, O., Stutzmann, J.J.M., Doble, A., and Blanchard, J.C. (1993) Altered synaptic plasticity and memory production in nitric oxide synthase inhibitor-treated rats. *Proc. Natl. Acad. Sci. USA* **90**, 9191-9194

51. Yamada, K., Noda, Y., Nakayama, S., Komori, Y., Sugihara, H., Hasegawa, T., and Nabeshima, T. (1995) Role of nitric oxide in learning and memory and in monoamine metabolism in the rat brain. *Br. J. Pharmacol*. **115**, 852-858

52. Yamada, K., Hiramatsu, M., Noda, Y., Mamiya, T., Murai, M., Kameyama, T., Komori, Y., Nikai, T., Sugihara, H., and Nabeshima, T. (1996) Role of nitric oxide and cyclic GMP in the dizocilpine-induced impairment of spontaneous alteration behavior in mice. *Neuroscience* **74**, 365-374

53. Kendrick, K.M., Guevara-Guzman, R., Zorrilla, J., Hinton, M.R., Broad, K.D., Mimmack, M., and Ohkura, S. (1997) Formation of olfactory memories mediated by nitric oxide. *Nature* **388**, 670-674

*Received November 21, 2000; revised January 31, 2001.*

**Fig. 1**

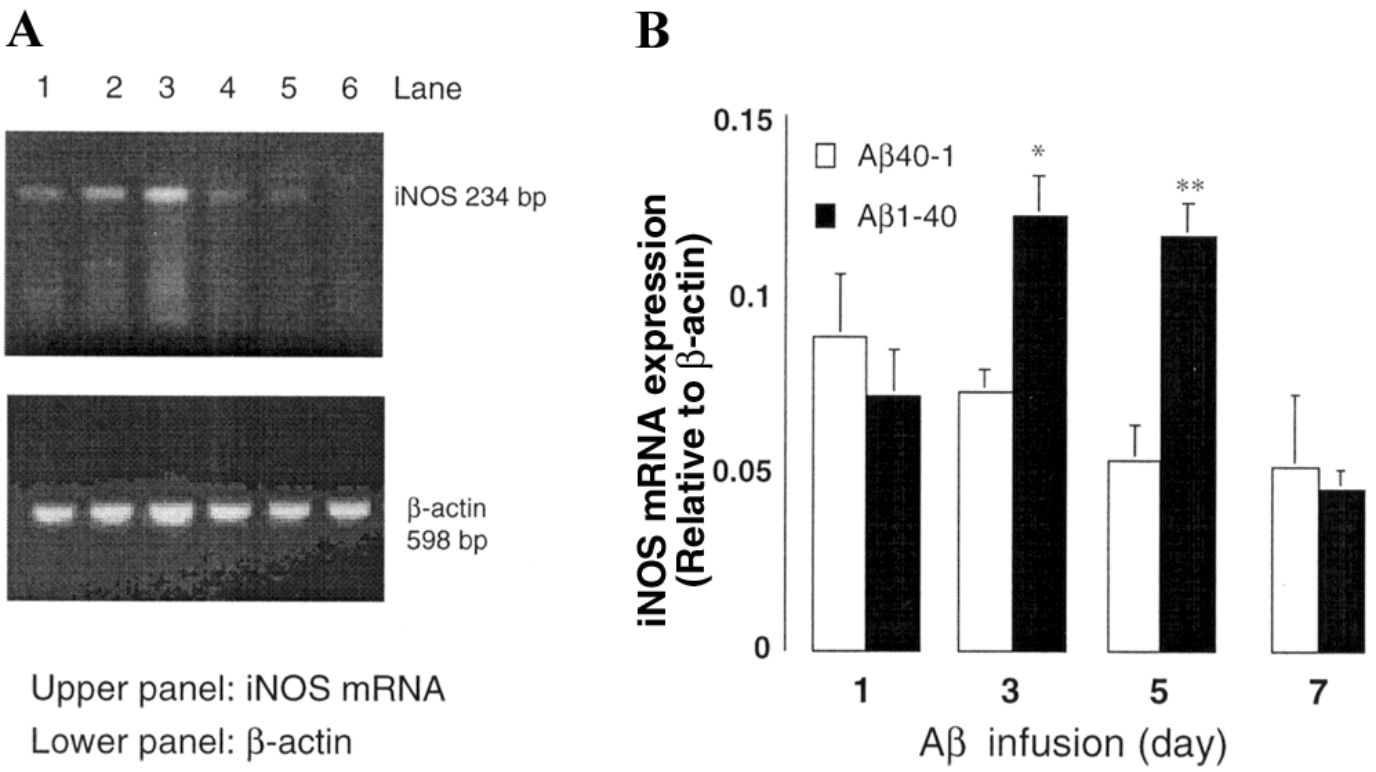


**Figure 1**. The expression of iNOS mRNA in rat hippocampus after continuous i.c.v. infusion with 300 pmol/day of Aβ1-40 or Aβ40-1 at different time points. Total RNA in the hippocampus was extracted, first-strand cDNA was synthesized, and iNOS expression was assessed by PCR as described in the text. β-Actin mRNA was assessed in all RNA samples as an internal control for the amount of RNA in each sample. **(A)** Expression of iNOS and β-actin was visualized by electrophoresis on 1.5% agarose. Lanes 1, 2, 3, and 4 represent the expression of iNOS after Aβ infusion for 1, 3, 5, and 7 days, respectively. Lanes 5 and 6 represent the expression of iNOS on day 5 in control (Aβ40-1) and naive rats, respectively. **(B)** iNOS expression was quantified relative to β-actin. Data were expressed as means ± SE for four rats in each group, with duplicate determinations. *$P < 0.05$, **$P < 0.01$ vs. Aβ40-1.

**Fig. 2**

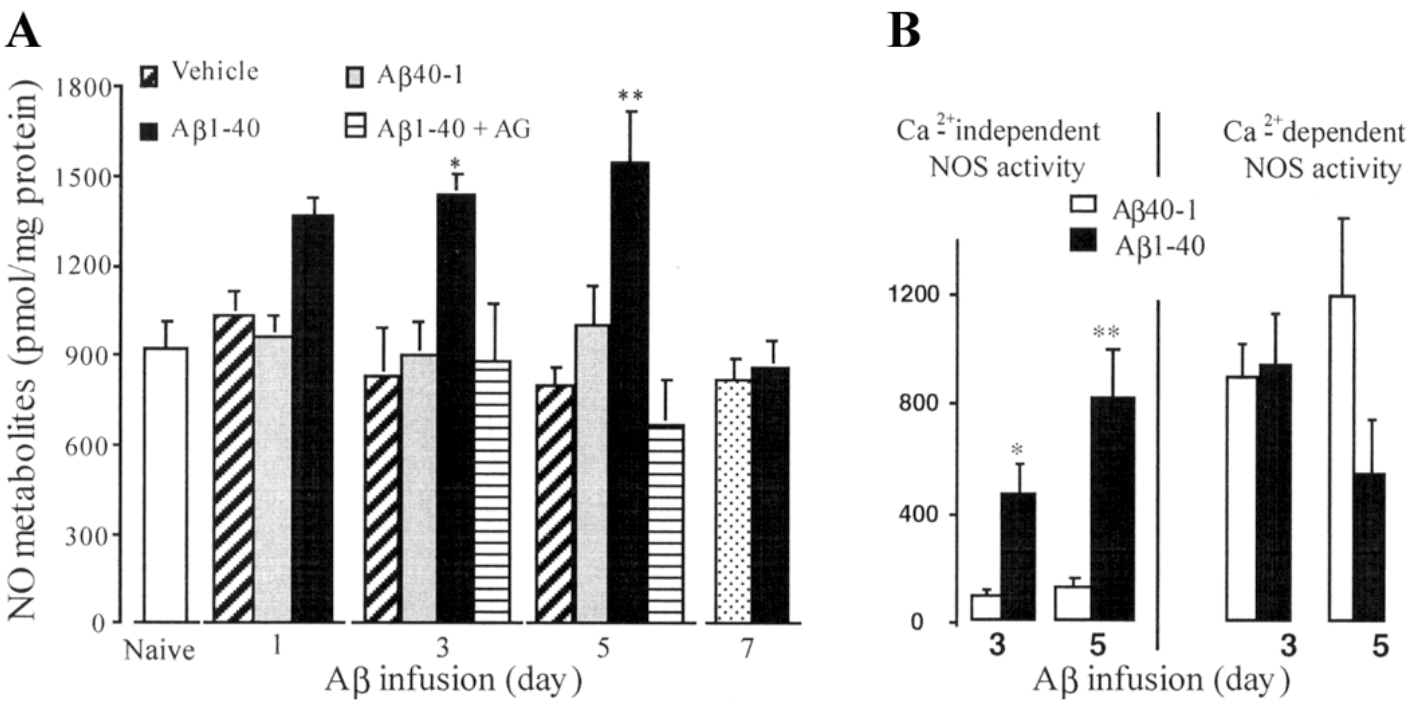


**Figure 2.** Accumulation of NO metabolites ($NO_x^-$) and increase in NOS activities in rat hippocampus after continuous i.c.v. infusion with 300 pmol/day of Aβ at different time points. **(A)** Accumulation of NO metabolites in the hippocampus and inhibitory effect of AG on NO metabolite accumulation. Daily treatment with AG (100 mg/kg, i.p.) abolished the increase in NO metabolite levels. **(B)** $Ca^{2+}$-independent and $Ca^{2+}$-dependent NOS activity in the hippocampus. Data were expressed as means ± SE for four rats in each group, with duplicate determinations. **P* < 0.05, ***P* < 0.01 vs. Aβ40-1.

**Fig. 3**

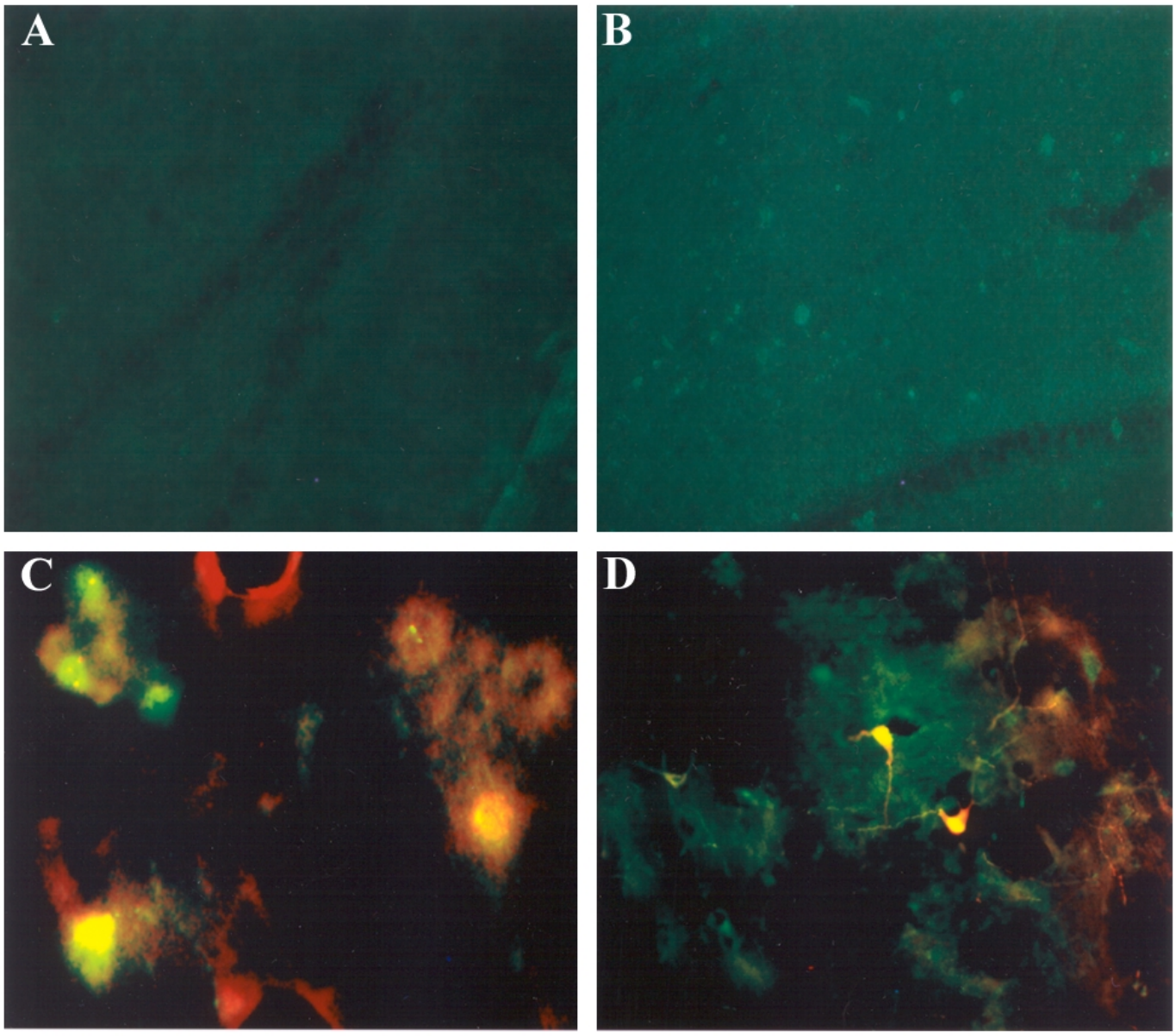


**Figure 3.** Immunofluorescent microscopic detection of iNOS-immunoreactive cells in rat hippocampus after a 5-day infusion of Aβ. Rat brain was cut into 30 μm thick sections and incubated with monoclonal mouse antibody against iNOS alone or in combination with either anti-GFAP or anti-CD11b antibodies. The sections were then incubated with secondary-conjugated antibodies. **(A)** Image obtained from the control (Aβ40-1), showing almost no immunoreactive cells. **(B)** Abundant iNOS-immunoreactive cells were found in the dentate gyrus of the hippocampus. **(C)** iNOS-immunoreactive cells (green) were colocalized with CD11b-immunopositive cells (red). **(D)** iNOS-immunoreactive cells (green) were colocalized with GFAP-immunopositive cells (orange).

**Fig. 4**

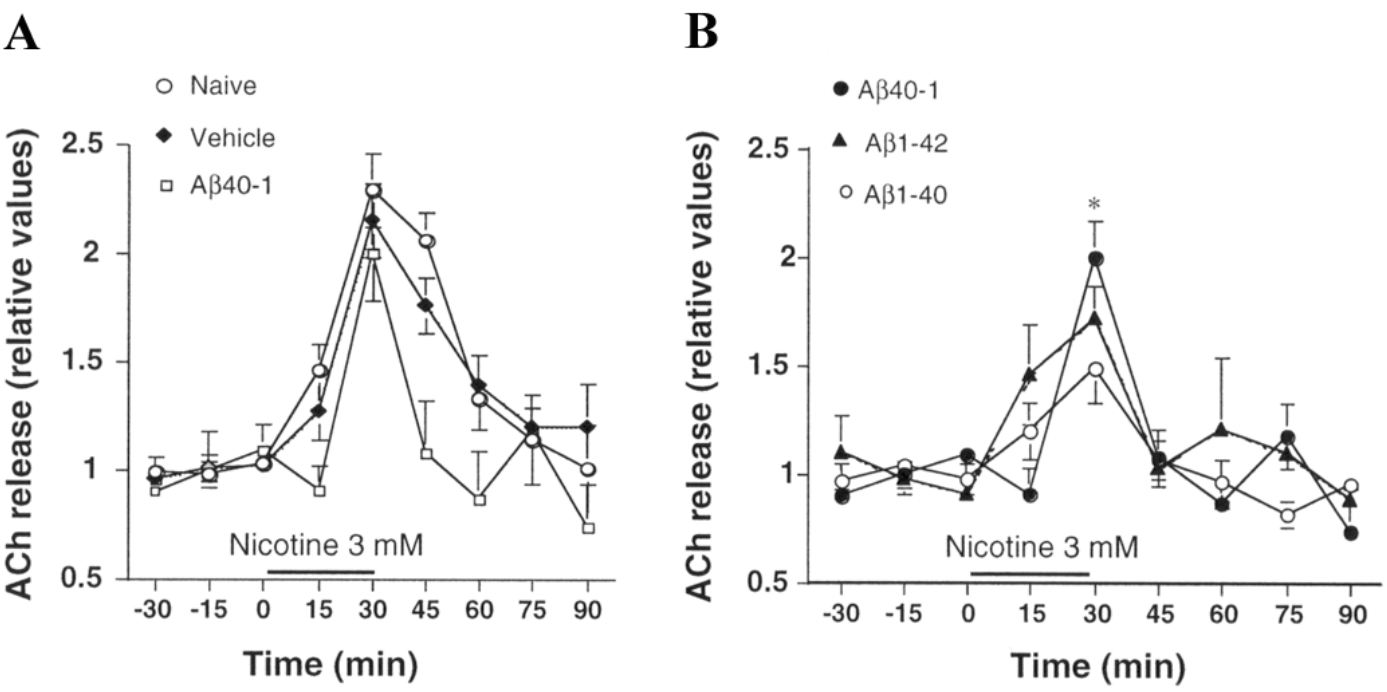


**Figure 4**. Effects of various Aβ fragments on nicotine-evoked ACh release in the frontal cortex and hippocampus. ACh release was measured on day 10 after Aβ infusion. The basal levels of ACh (pmol/60 μl/15 min) in the dialysate were **(A)** 0.36 ± 0.04 in naive rats ($n$ = 4), 0.28 ± 0.07 in vehicle-infused rats ($n$ = 5), 0.33 ± 0.04 in Aβ40-1-infused rats ($n$ = 5), and **(B)** 0.38 ± 0.08 in Aβ1-40-infused rats ($n$ = 7) and 0.28 ± 0.08 in Aβ1-42-infused rats ($n$ = 6). Data were expressed as means ± SE. *$P$ < 0.05 vs. Aβ40-1 (Bonferroni post-hoc test).

**Fig. 5**

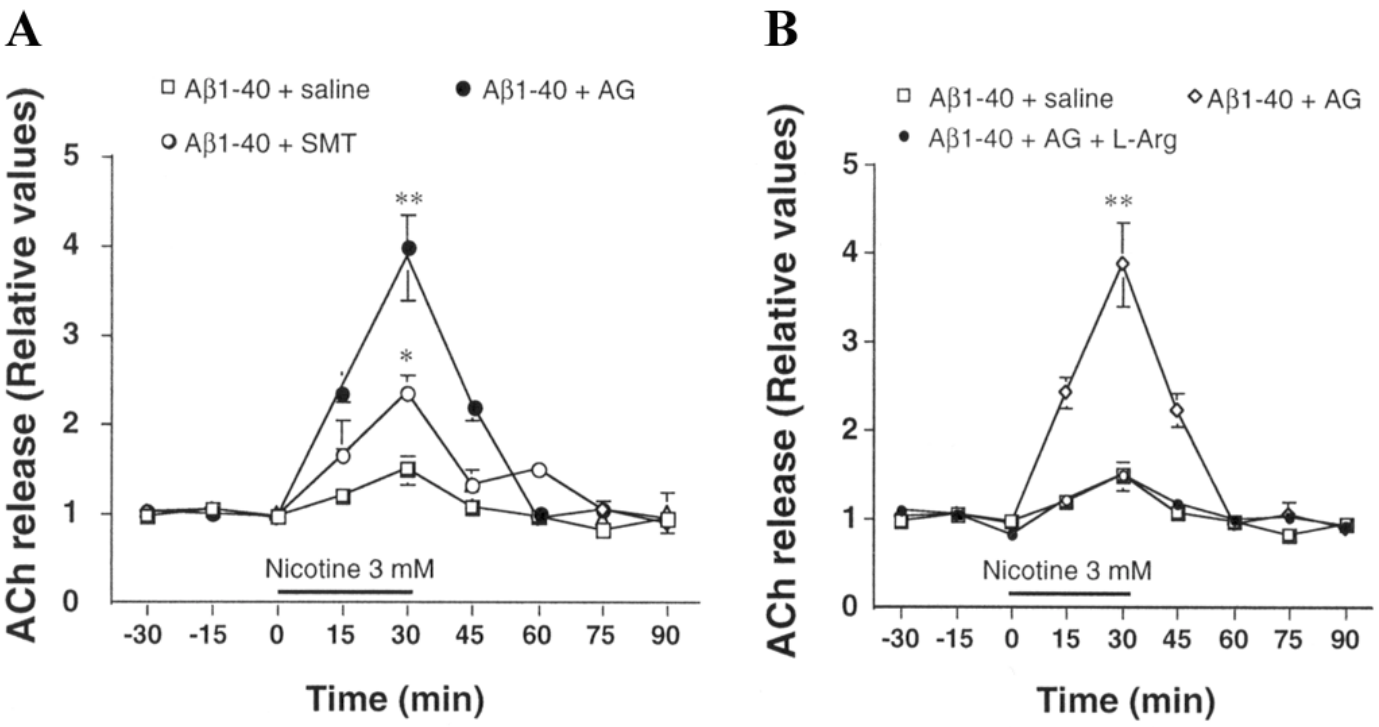


**Figure 5**. Effects of iNOS and nNOS inhibitors on Aβ-induced impairment of nicotine-evoked ACh release in the frontal cortex and hippocampus. ACh release was measured on day 10 after Aβ infusion. The basal levels of ACh (pmol/60 µl/15 min) in the dialysate were **(A)** 0.35 ± 0.07 in the Aβ1-40 + saline group ($n$ = 6), 0.22 ± 0.09 in the Aβ1-40 + SMT group ($n$ = 7), 1.19 ± 0.41 in the Aβ1-40 + AG group ($n$ = 6), and **(B)** 1.19 ± 0.41 in the Aβ1-40 + AG group ($n$ = 6) and 0.79 ± 0.14 in the Aβ1-40 + AG + L-Arg group ($n$ = 5). Data were expressed as means ± SE. *$P$ < 0.05, **$P$ < 0.01 vs. Aβ1-40 + saline (Bonferroni post-hoc test).

**Fig. 6**

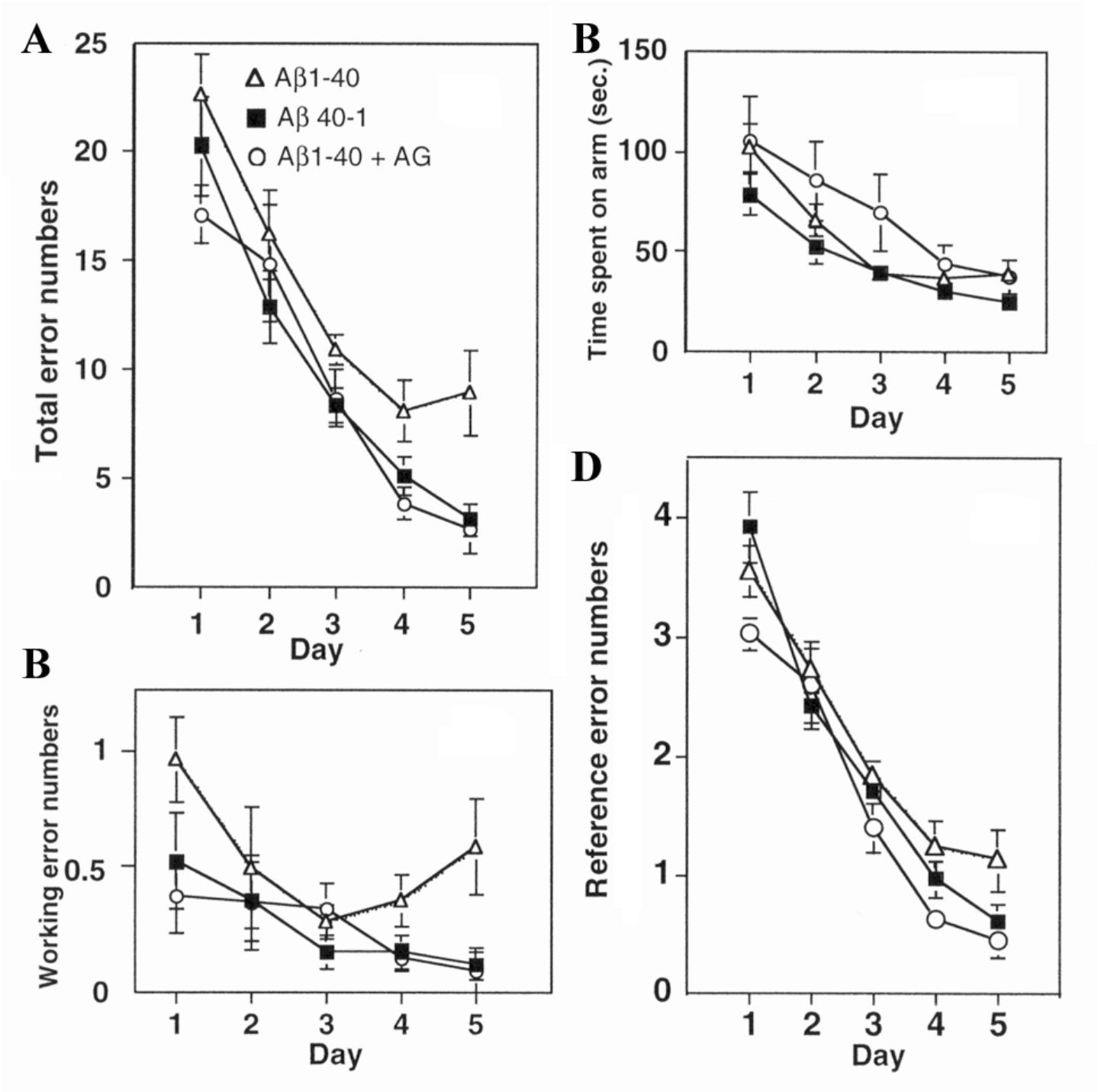


**Figure 6.** Effects of AG on Aβ-induced impairment of learning in an eight-arm radial maze task. The maze training (5 trials/day) was carried out on days 10-14 after i.c.v. infusion of Aβ. **(A)** Total memory error. **(B)** Time spent on arm. **(C)** Working memory error. **(D)** Reference memory error. Data were expressed as means ± SE. The number of animals in each group was eight for Aβ40-1, nine for Aβ1-40, and seven for Aβ1-40 + AG. Aβ1-40 significantly impaired spatial memory formation (A, $P<0.01$), as well as working and reference memory formation (C, $P<0.05$; D, $P<0.01$, respectively), but not locomotor function (B). AG significantly prevented Aβ-induced impairment of spatial memory formation (A, $P<0.005$; C, $P<0.05$; and D, $P<0.002$).